# Evaluation of Starting Current of Induction Motors Using Artificial Neural Network

**Iman Sadeghkhani[(1)] - Alireza Sadoughi[(2)]**
(1) Ph.D. Candidate - Department of Electrical and Computer Engineering, Isfahan University of Technology
(2) Assistant Professor - Department of Electrical Engineering, Malek-Ashtar University of Technology

Received: 2014/1/27 Accepted: 2014/8/16

Induction motors (IMs) are widely used in industry including it be an electrical or not. However during starting period, their starting currents are so large that can damage equipment. Therefore, this current should be estimated accurately to prevent hazards caused by it. In this paper, the artificial neural network (ANN) as an intelligent tool is used to evaluate starting current peak of IMs. Both Multilayer Perceptron (MLP) and Radial Basis Function (RBF) structures have been analyzed. Six learning algorithms, backpropagation (BP), delta-bar-delta (DBD), extended delta-bar-delta (EDBD), directed random search (DRS), quick propagation (QP), and levenberg marquardt (LM) were used to train the MLP. The simulation results using MATLAB show that most developed ANNs can estimate the starting current peak of IMs with good accuracy. However, it is proven that LM and EDBD algorithms present better performance for starting current evaluation based on average of relative and absolute errors.

**Index Terms**: Induction motors, multilayer perceptron, radial basis function, starting current.

**Nomenclature**

| | |
|---|---|
| $V_{ds}$ , $V_{qs}$ | direct/quadrature component of stator voltage |
| $V'_{dr}$ , $V'_{qr}$ * | direct/quadrature component of rotor voltage |
| $i_{ds}, i_{qs}$ | direct/quadrature component of stator current |
| $i'_{dr}, i'_{qr}$ | direct/quadrature component of rotor current |
| $R_s$ , $L_{ls}$ | stator winding resistance and inductance |
| $R'_r$ , $L'_{lr}$ | rotor winding resistance and inductance |
| $L_m$ | magnetizing inductance |
| $\varphi_{ds}$ , $\varphi_{qs}$ | direct/quadrature component of stator flux |
| $\varphi'_{dr}$ , $\varphi'_{qr}$ | direct/quadrature component of rotor flux |
| $L_s$ , $L'_r$ | total stator and rotor inductances |
| $T_e$ | electromagnetic torque |
| $T_L$ | shaft load torque |
| $\omega_m$ | angular velocity of the rotor |
| $\theta_m$ | rotor angular position |
| $\omega_r$ | electrical angular velocity |
| p | number of pole pairs |
| J | combined rotor and load inertia coefficient |
| B | combined rotor and load viscous friction coefficient |
| $R_c$ , $L_c$ | cable resistance and inductance |

* Prime signs show that all parameters are referred to the stator.

**Corresponding Author:** Iman Sadeghkhani - Najafabad Branch, Islamic Azad University, i.sadeghkhani@ec.iut.ac.ir

## 1. Introduction

Induction Motor (IM), also called asynchronous motor, is the most common motor in various sections of the world including industrial, domestic, educational sections, etc. [1], [2]. Single phase IMs are commonly used in household applications, while three-phase ones are widely used in industry. Three-phase IMs are cheap, robust, efficient and reliable; also they have low maintenance cost and high starting torque. In addition, their range is wide (from a few watts to values on the order of 10000 hp) and their speed is nearly constant. In contrast, speed control of IMs is not easy and they have low power factor (lagging) in the lightly loaded condition. Moreover, their starting current may be five to ten times the full-load current [3], [4].

As mentioned above, IMs are very important equipment in the industry. Without induction motors, many products cannot be produced by manufactures and human's life is disrupted. But one of the disadvantages of IMs is the high starting current which can damage stator windings and fluctuate grid voltage. Also, there is need to higher range of switches and equipment. This high starting current is more notable in the high-power IMs. Therefore, this current must be estimated accurately to prevent above problems. Usually, starting current of IMs are estimated based on experimental data from the tests or by calculation in the design stage. In [5], a genetic algorithm is used to estimate IM parameters. Also, parameters of Induction motors are estimated using transient stator current in [6]. Moreover, stator current discharge is used in [7] to estimate parameters of single-phase axial flux induction motors. Also, a non-linear optimization routine-based method is proposed to estimate IM parameters in [8]. In [9], parameters of IM are estimated using current envelope. Also, extended kalman filtering algorithm is proposed to estimate state and parameters of IMs in [10].

This paper presents an intelligent approach to evaluate starting current of induction motors in the design stage or operation situation considering aging effects on the equipment (motor and cable) parameters. Also, this intelligent estimator includes cable effect on the starting current of IMs [5], [6].

In this paper power system blockset (PSB), a MATLAB/Simulink-based simulation tool, is used for calculation of starting current of IMs [7]. In order to study various conditions of starting an IM, many possible system configurations must be considered which needs many time-domain simulations resulting in a large amount of simulation time. This paper presents a real-time estimator for starting current of IMs. The Artificial Neural Network (ANN) is used as intelligent tool for this purpose. A tool such as proposed in this paper that can give the starting current peak will be helpful to the manufactures during design stage and to the operators during operation condition. The ANN is trained with the most common structures. In the proposed estimator, we have considered the most important aspects which influence the starting current peak such as supply voltage, cable resistance and reactance, stator/rotor resistance and reactance, magnetizing reactance, and switching angle. This information will help the companies and operators to design and handle IMs safely with starting current appearing safe within the limits. Results of the studies shows that developed ANNs can estimate starting current of induction motors with excellent accuracy.

## 2. Study of System Modelling

### A. Induction Machine

The electrical section of IM is represented by a fourth-order state-space model and the mechanical section by a second-order system [8]. All electrical variables and parameters are referred to the stator. All stator and rotor quantities are in the arbitrary two-axis reference frame (d-q frame). Equivalent circuit of an induction machine is shown in Fig. (1) Electrical equations for the stator and rotor circuits of the induction machine described in d- and q-axes are as follows.

$$V_{qs} = R_s i_{qs} + \frac{d}{dt}\varphi_{qs} + \omega\varphi_{ds} \quad (1)$$

$$V_{ds} = R_s i_{ds} + \frac{d}{dt}\varphi_{ds} - \omega\varphi_{qs} \quad (2)$$

$$V'_{qr} = R'_r i'_{qr} + \frac{d}{dt}\varphi'_{qr} + (\omega - \omega_r)\varphi'_{dr} \quad (3)$$

$$V'_{dr} = R'_r i'_{dr} + \frac{d}{dt}\varphi'_{dr} - (\omega - \omega_r)\varphi'_{qr} \quad (4)$$

$$T_e = \frac{3}{2}p(\varphi_{ds} i_{qs} - \varphi_{qs} i_{ds}) \quad (5)$$

where:

$$\varphi_{qs} = L_s i_{qs} + L_m i'_{qr} \quad (6)$$

$$\varphi_{ds} = L_s i_{ds} + L_m i'_{dr} \quad (7)$$

$$\varphi'_{qr} = L'_r i'_{qr} + L_m i'_{qs} \quad (8)$$

$$\varphi'_{dr} = L'_r i'_{dr} + L_m i'_{ds} \quad (9)$$

$$L_s = L_{ls} + L_m \quad (10)$$

$$L'_r = L'_{lr} + L_m \quad (11)$$

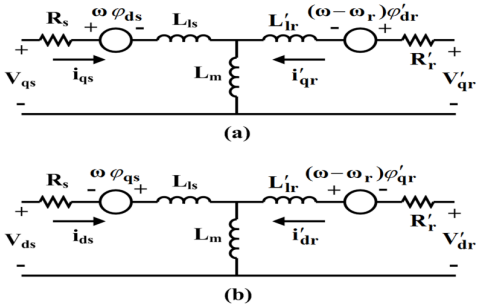


Fig. (1): Equivalent circuit of induction machine; (a) q-axis, (b) d-axis

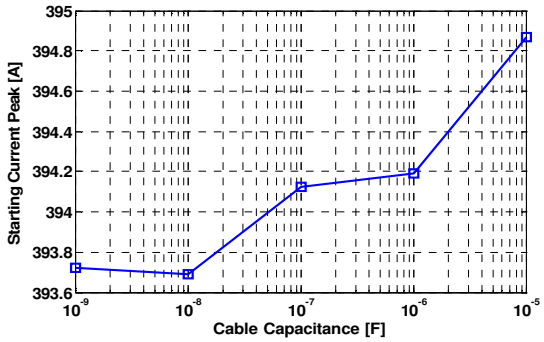


Fig. (2): Effect of cable capacitance on the starting current peak

Also, mechanical part equations are:

### B. Connecting Cable

Usually cables are modeled using series resistance and inductance and parallel capacitance in the distributed form or in the PI form [9]. As shown in Fig. 2, cable capacitance has negligible effect on the starting current peak. Thus, in this work cable capacitance has been neglected. This capacitor must be used for the long cable or for the transient studies of induction machines where it isn't negligible [10]. Therefore, connecting cable is modeled by a series equivalent resistance and reactance.

## 3. Study of Stating Current

The electric motive force (EMF) induced in the rotor depends on relative speed of rotor shaft and synchronous speed. Since in the starting condition the motor is standstill, this relative speed has its maximum value and therefore large EMF is induced in the rotor. When an induction motor is stationary, it behaves like a transformer which its secondary winding is short circuited. This causes low impedance to the system voltage and hence IM draws a high current from the gird, typically 5-10 times full-load current.

Motor load doesn't affect starting current peak; although the inertia of the motor and load must be overcome. If inertia is big, the motor takes more time to reach full speed. When the motor accelerates, part of the starting current power overcomes this inertia and is converted to kinetic energy. The remaining power of the starting current heats the rotor, up to possibly 250°C for a "long" starting (20 seconds).

The sample system considered for explanation of the proposed methodology consists a high-power induction motor which produces notable starting current. This system is shown in Fig. 3. For this purpose, induction motor KHV355-2 from VALIADIS company was considered [11]. It is a 200 kW (270 hp), 3300 V induction motor which is in the high-power/medium-voltage category. Parameters of this motor were calculated using no-load test, locked-rotor test, and DC test [12]. This motor is fully simulated in the MATLAB software [7]. Fig. 4 shows stator currents of this motor.

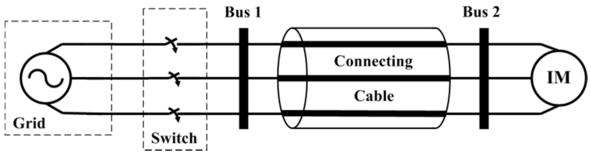


Fig. (3): Sample system for the starting current study

In practical system a number of factors affect the starting current peak. In this paper following parameters were considered:

- Supply Voltage (V )
- Equivalent resistance of the connecting cable ($R_c$)
- Equivalent reactance of the connecting cable ($X_c$)
- Stator resistance ($R_s$)
- Stator reactance ( $X_{ls}$)
- Rotor resistance ($R'_r$)
- Rotor reactance ( $X'_{lr}$)
- Magnetizing reactance ( $X_m$)
- Switching angle ( S.A.)

Stator reactance affects the starting current. Fig. 5 shows the effect of stator reactance on the starting current peak at different rotor resistance. Starting current peak is the maximum of stator current peaks between all three phases. Fig. 6 shows the effect of cable resistance on the starting current peak at different supply voltage. Fig. 7 presents effect of stator resistance on the starting current peak at different rotor reactance. Fig. 8 shows the effect of magnetizing reactance on the starting current peak at different stator resistance. Finally, effect of switching angle on the starting current peak has been shown in Fig. 9.

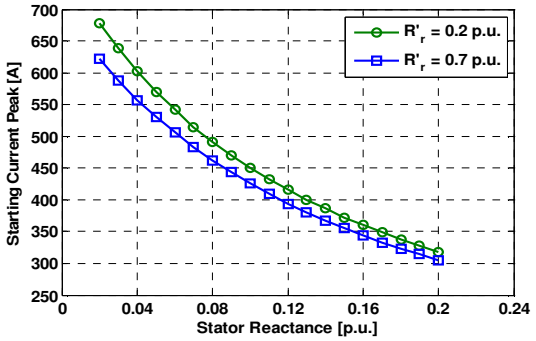


Fig. (5): Starting current peak as stator reactance while supply voltage 1 p.u., cable resistance 0.004 p.u., cable reactance 0.0126 p.u., stator resistance 0.012 p.u., referred rotor reactance 0.1 p.u., magnetizing reactance 2 p.u., and switching angle 0°

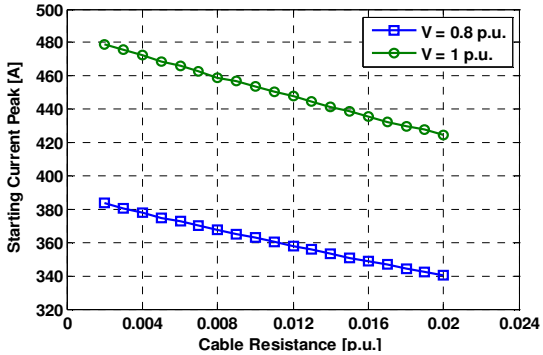


Fig. (6): Starting current peak as cable resistance while cable reactance 0.0126 p.u., stator resistance 0.012 p.u., stator reactance 0.08 p.u., referred rotor resistance 0.01 p.u., referred rotor reactance 0.1 p.u., magnetizing reactance 2.2 p.u., and switching angle 0°.

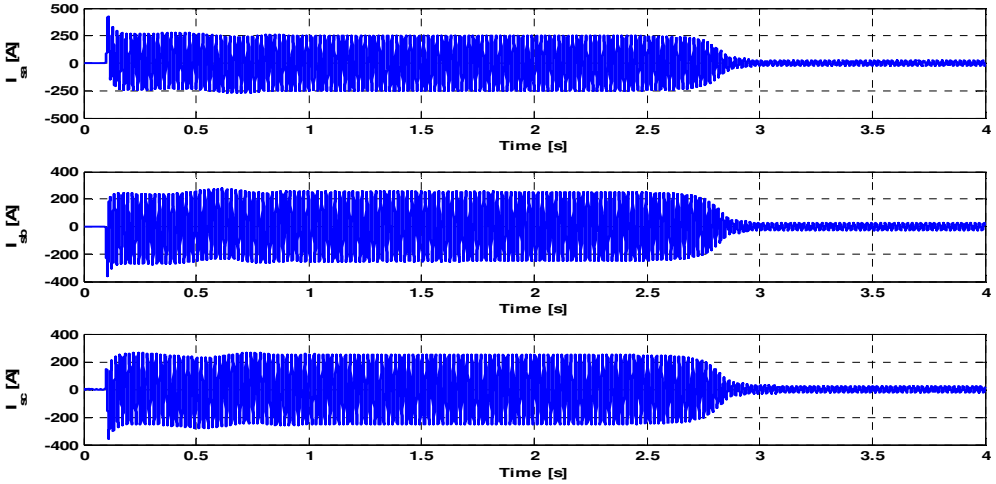


Fig. (4): Stator currents of an induction motor

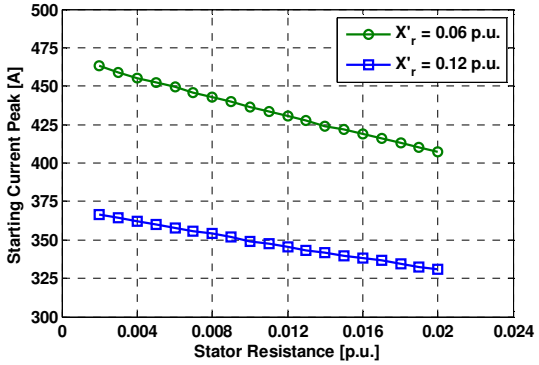


Fig. (7): Starting current peak as stator resistance while supply voltage 0.9 p.u., cable resistance 0.006 p.u., cable reactance 0.0063 p.u., stator reactance 0.12 p.u., referred rotor resistance 0.008 p.u., magnetizing reactance 2.3 p.u., and switching angle 0°

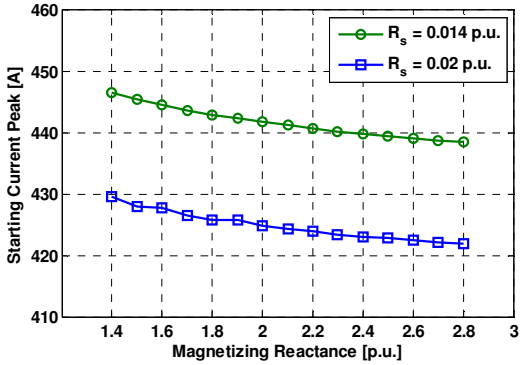


Fig. (8): Starting current peak as magnetizing reactance while supply voltage 1 p.u., cable resistance 0.002 p.u., cable reactance 0.0063 p.u., stator reactance 0.1 p.u., referred rotor resistance 0.012 p.u., referred rotor reactance 0.1 p.u., and switching angle 0°

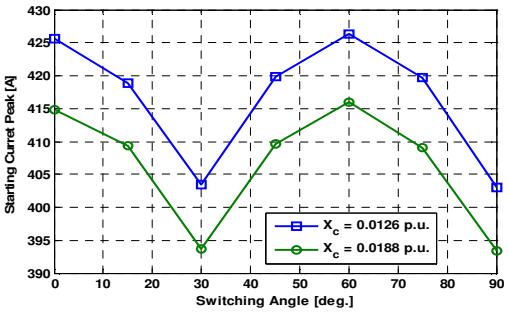


Fig. (9): Starting current peak as switching angle while supply voltage 1 p.u., cable resistance 0.004 p.u., stator resistance 0.012 p.u., stator reactance 0.1 p.u., referred rotor resistance 0.014 p.u., referred rotor reactance 0.1 p.u., and magnetizing reactance 2 p.u

## 4. The Artificial Neural Network

There are many types of neural networks for various applications available in the literature [13-17]. Multilayer Perceptrons (MLPs) and Radial Basis Functions (RBFs) are examples of feed-forward networks and both universal approximators. In spite of being different networks in several important respects, these two neural network architectures are capable of accurately mimicking each other.

In this work, different algorithms were used to train MLP structure: Back Propagation (BP), Delta-Bar-Delta (DBD), Extended Delta-Bar-Delta (EDBD), Directed Random. Search (DRS), Quick Propagation (QP), and Levenberg–Marquardt (LM). Because of space limitation, these structures and related algorithms are not described here; detailed structure of BP, DBD, EDBD, DRS, QP, and RBF are presented in [13], and LM algorithm is fully discussed in [18]. The basic structure of developed artificial neural network is shown in Fig. 10.

### a) Training of Artificial Neural Network

Parameters listed in Section 3 are adopted as ANN inputs and starting current peak is ANN output. To train ANNs, all experiments have been repeated for different system parameters. For producing learning and testing sets, ANN inputs were varied in different steps (depend on the parameter). 10% of these sets were used for ANN learning and 90% of these sets were used for ANN testing. Each ANN is trained with the goal of mean square error (MSE) 1e-6. Fig. 11 shows the training of developed neural networks. Specifications of ANNs are presented in Table 1. After learning, all parameters of the trained networks have been frozen and then used in the retrieval mode for testing the capabilities of the system on the data not used in learning. The testing data samples have been generated through the PSB program by placing the parameter values not used in learning, by applying different parameters. A large number of testing data have been used to check the proposed solution in the most objective way at practically all possible parameters variation. Relative error is calculated by the difference of PSB output and ANN output:

$$\mathrm{Er}_{\mathrm{Relative}}\ (\%) = \frac{\left|\mathrm{I}_{\mathrm{ANN}} - \mathrm{I}_{\mathrm{PSB}}\right|}{\mathrm{I}_{\mathrm{PSB}}} \times 100 \qquad (14)$$

and absolute error is calculated as:

$$\mathrm{Er}_{\mathrm{Absolute}} = \left|\mathrm{I}_{\mathrm{ANN}} - \mathrm{I}_{\mathrm{PSB}}\right| \qquad (15)$$

where $I_{ANN}$ is starting current peak calculated by ANN, and $I_{PSB}$ refers to starting current peak calculated by PSB.

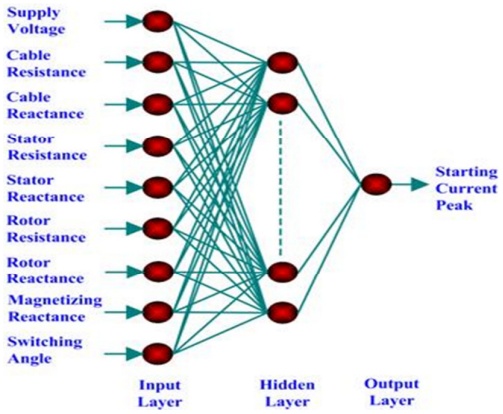


Fig. (10): Basic structure of developed artificial neural network

Table (1): Specifications of developed ANNs

| ANN model | Number of neurons in the hidden layer | Training time [epochs] |
|---|---|---|
| **BP** | 5 | 178 |
| **DBD** | 7 | 1189 |
| **EDBD** | 8 | 315 |
| **DRS** | 6 | 109 |
| **LM** | 6 | 286 |
| **QP** | 7 | 975 |
| **RBF** | 5 | 354 |

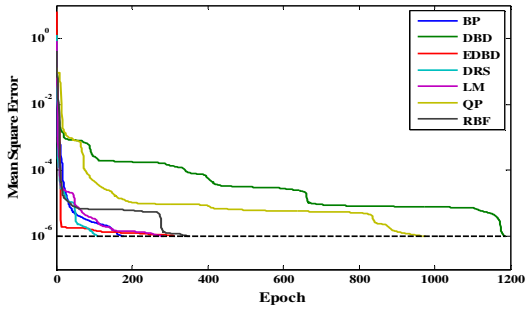


Fig. (11): Squared error against epoch curve for developed ANNs

Fig. 12 shows relative errors for LM algorithm. Moreover, results for a sample test data for all developed ANNs are presented in Table 2 and Figs. 13-15. Calculated errors for different ANNs in Table 2 are relative errors. Fig. 13 shows starting current peak against the supply voltage, Fig. 14 presents starting current peak against the cable reactance, and Fig. 15 shows starting current peak against the stator resistance.

## 5. Discussion

In this paper, starting current peak was evaluated using BP, DBD, EDBD, DRS, QP, LM and RBF neural networks. To select best approach for starting current evaluation, a comparison has been made. Table 3 presents a comparison between these methods based on average of relative and absolute errors for Table 2 sample data. It can be seen from Table 3 that LM and EDBD algorithms have better performance (smaller relative and absolute errors) to evaluate starting current peak in the induction motors.

## 6. Conclusion

This paper presents an artificial neural network-based approach to evaluate starting current peak of induction motors including cable effect. Both MLP and RBF structures have been employed for this purpose. MLP is trained with BP, DBD, EDBD, DRS, QP, and LM algorithms. Simulation results show that most developed ANNs can estimate starting current; however LM and EDBD algorithms present better accuracy. This technique can help the companies and operators to evaluate starting current peak during both design and operation stages in real-time.

## Acknowledgment

This work has been supported by the Iran's National Elites Foundation.

Table (3): Average of Relative and Absolute Errors for Table (2) Sample Data

| ANN Model | Average of Relative Error [%] | Average of Absolute Error [A] |
|---|---|---|
| **LM** | 0.0922 | 0.4034 |
| **EDBD** | 0.1272 | 0.5797 |
| **BP** | 0.1824 | 0.7716 |
| **DBD** | 0.2114 | 0.9137 |
| **QP** | 0.4066 | 1.7282 |
| **RBF** | 0.7624 | 3.3372 |
| **DRS** | 1.9902 | 8.9127 |

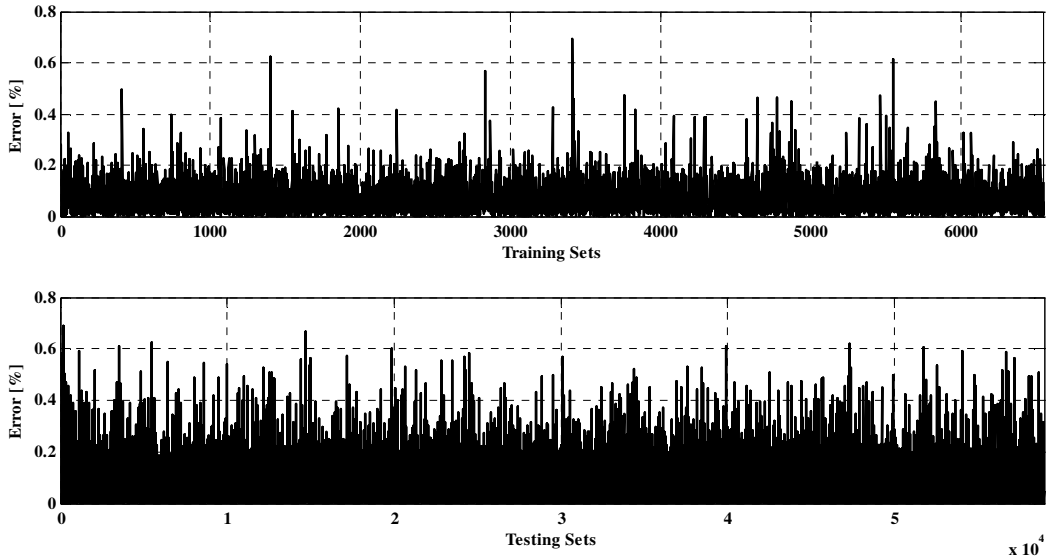


Fig. (12): Relative errors of learning and testing sets for LM algorithm

Table (2): Some Sample Testing Data and Output

| V | 0.8 | 0.8 | 0.8 | 0.8 | 0.9 | 0.9 | 0.9 | 0.9 | 1 | 1 | 1 | 1 | 1.1 | 1.1 | 1.1 | 1.1 |
|---|---|---|---|---|---|---|---|---|---|---|---|---|---|---|---|---|
| $R_c$ | 0.6 | 0.6 | 0.6 | 0.6 | 0.2 | 0.2 | 0.2 | 0.2 | 0.3 | 0.4 | 0.5 | 0.6 | 0.3 | 0.3 | 0.3 | 0.3 |
| $X_c$ | 0.0314 | 0.0314 | 0.0314 | 0.0314 | 0.0189 | 0.0251 | 0.0314 | 0.0377 | 0.0251 | 0.0251 | 0.0251 | 0.0251 | 0.0314 | 0.0314 | 0.0314 | 0.0314 |
| $R_s$ | 0.5 | 0.4 | 0.4 | 0.5 | 0.6 | 0.6 | 0.6 | 0.6 | 0.5 | 0.5 | 0.5 | 0.5 | 0.4 | 0.5 | 0.6 | 0.7 |
| $X_{ls}$ | 4 | 4 | 4 | 4 | 3 | 4 | 5 | 6 | 5 | 5 | 5 | 5 | 4 | 4 | 4 | 4 |
| $R'_r$ | 0.4 | 0.4 | 0.4 | 0.4 | 0.4 | 0.6 | 0.6 | 0.4 | 0.4 | 0.5 | 0.6 | 0.7 | 0.6 | 0.6 | 0.6 | 0.6 |
| $X'_{lr}$ | 3 | 4 | 5 | 6 | 5 | 5 | 5 | 5 | 5 | 5 | 5 | 5 | 3 | 3 | 3 | 3 |
| $X_m$ | 110 | 110 | 110 | 110 | 90 | 100 | 110 | 120 | 100 | 100 | 100 | 100 | 110 | 110 | 110 | 110 |
| S.A.[°] | 10 | 10 | 10 | 10 | 30 | 30 | 30 | 30 | 55 | 55 | 55 | 55 | 80 | 80 | 80 | 80 |
| PSB | 409.3465 | 381.927 | 354.2365 | 327.2188 | 459.0562 | 398.871 | 368.4783 | 344.466 | 420.7591 | 411.5882 | 403.1649 | 395.2277 | 581.0046 | 573.7519 | 566.5372 | 559.391 |
| LM | 409.5152 | 382.5548 | 354.1394 | 326.7324 | 458.6114 | 398.1558 | 368.4264 | 344.7404 | 420.8398 | 412.3009 | 403.1615 | 394.6765 | 580.1499 | 572.8548 | 566.4511 | 559.7936 |
| Error | 0.041216 | 0.164401 | 0.027428 | 0.148647 | 0.096902 | 0.179304 | 0.014072 | 0.079682 | 0.019197 | 0.173142 | 0.000834 | 0.139484 | 0.147115 | 0.156365 | 0.015198 | 0.071961 |
| EDBD | 408.9137 | 382.0169 | 354.7666 | 327.604 | 458.2575 | 399.5689 | 369.0665 | 344.4949 | 420.8314 | 411.2594 | 403.6999 | 395.8744 | 581.5967 | 572.5757 | 567.5547 | 560.7457 |
| Error | 0.105721 | 0.023557 | 0.149631 | 0.117731 | 0.173987 | 0.174972 | 0.159633 | 0.008401 | 0.017202 | 0.0799 | 0.132716 | 0.163611 | 0.101905 | 0.204995 | 0.17959 | 0.242162 |
| BP | 408.3079 | 382.1378 | 355.2442 | 326.1499 | 458.2769 | 397.707 | 369.1933 | 344.6419 | 420.4815 | 411.0355 | 402.1688 | 396.3045 | 579.49 | 573.1488 | 565.5388 | 559.5571 |
| Error | 0.253722 | 0.055194 | 0.284454 | 0.326658 | 0.16976 | 0.291813 | 0.194049 | 0.051068 | 0.065955 | 0.134295 | 0.247073 | 0.272443 | 0.260688 | 0.105113 | 0.176241 | 0.029684 |
| DBD | 409.0761 | 383.1141 | 352.9714 | 327.6894 | 460.3465 | 399.352 | 369.2799 | 343.2903 | 419.7283 | 412.1541 | 402.6703 | 395.9611 | 579.9978 | 574.5978 | 567.8341 | 561.0941 |
| Error | 0.066065 | 0.310826 | 0.357156 | 0.143818 | 0.28107 | 0.120601 | 0.217558 | 0.341294 | 0.244971 | 0.137478 | 0.122682 | 0.185563 | 0.173285 | 0.147439 | 0.228911 | 0.304444 |
| QP | 411.2067 | 379.5639 | 351.7518 | 325.8739 | 462.351 | 400.4607 | 367.1107 | 345.2861 | 422.0617 | 410.1308 | 402.9587 | 392.7016 | 581.275 | 575.5538 | 569.9091 | 557.802 |
| Error | 0.454422 | 0.618711 | 0.70144 | 0.411004 | 0.717732 | 0.39855 | 0.37113 | 0.238091 | 0.309601 | 0.354101 | 0.051147 | 0.639172 | 0.046536 | 0.314053 | 0.595173 | 0.284065 |
| RBF | 407.6599 | 380.965 | 358.8303 | 326.9064 | 462.7908 | 395.313 | 371.838 | 348.6356 | 421.0887 | 416.2951 | 400.1795 | 399.0697 | 579.2769 | 569.388 | 572.1093 | 551.9008 |
| Error | 0.412024 | 0.251881 | 1.296812 | 0.095453 | 0.813531 | 0.892012 | 0.911777 | 1.210471 | 0.078334 | 1.143597 | 0.740491 | 0.972091 | 0.297367 | 0.760592 | 0.983528 | 1.339008 |
| DRS | 412.7117 | 373.4804 | 343.9103 | 328.1574 | 474.2285 | 399.2976 | 378.9444 | 354.2537 | 420.0458 | 403.9491 | 416.0935 | 399.5476 | 596.9357 | 585.4837 | 551.3274 | 574.591 |
| Error | 0.822075 | 2.211562 | 2.915072 | 0.28686 | 3.305103 | 0.106964 | 2.840375 | 2.841425 | 0.169516 | 1.856013 | 3.206777 | 1.093008 | 2.741987 | 2.044756 | 2.68471 | 2.717229 |

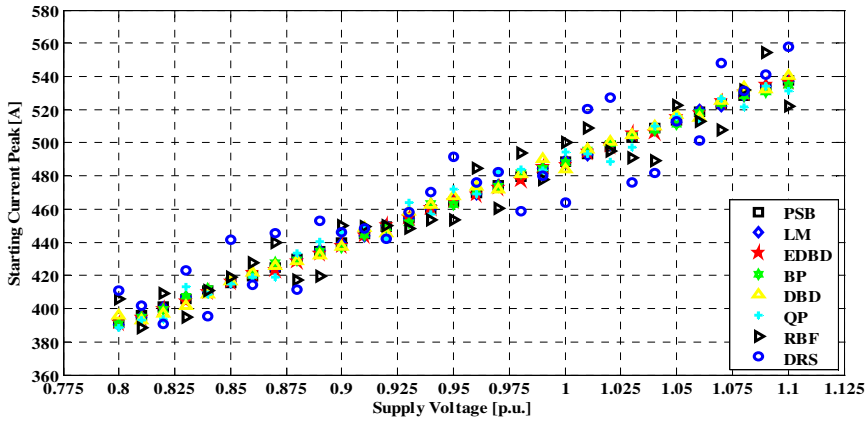


Fig. (13): Starting current peak vs. supply voltage simulated by ANNs and PSB while cable resistance 0.006 p.u., cable reactance 0.0188 p.u., stator resistance 0.012 p.u., stator reactance 0.06 p.u., referred rotor resistance 0.012 p.u., referred rotor reactance 0.1 p.u., magnetizing reactance 2.2 p.u., and switching angle 0°

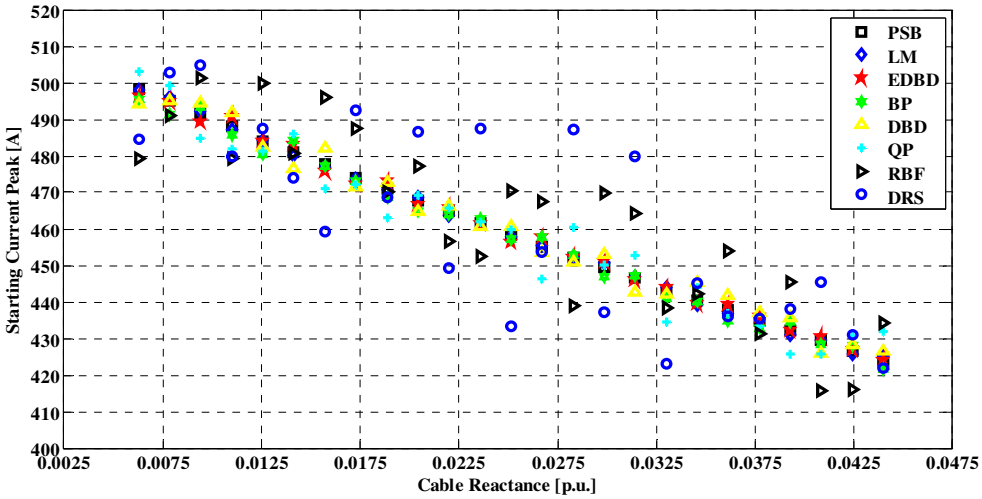


Fig. (14): Starting current peak vs. cable reactance simulated by ANNs and PSB while supply voltage 1 p.u., cable resistance 0.004 p.u., stator resistance 0.01 p.u., stator reactance 0.08 p.u., referred rotor resistance 0.008 p.u., referred rotor reactance 0.1 p.u., magnetizing reactance 2.4 p.u., and switching angle 0°

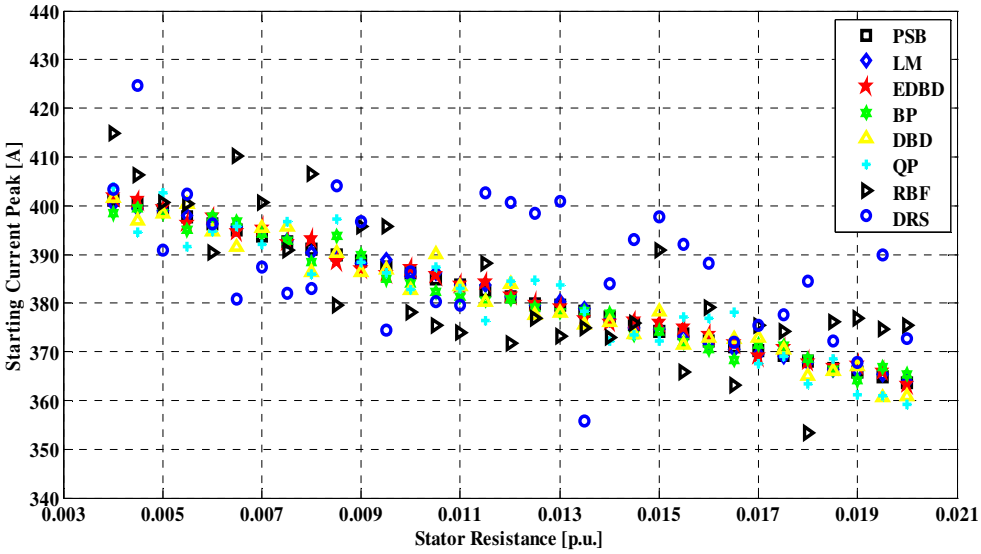


Fig. (15): Starting current peak vs. stator resistance simulated by ANNs and PSB while supply voltage 0.9 p.u., cable resistance 0.002 p.u., cable reactance 0.0188 p.u., stator reactance 0.1 p.u., referred rotor resistance 0.012 p.u., referred rotor reactance 0.1 p.u., magnetizing reactance 2.2 p.u., and switching angle 0°

## References

[1] M. Ito, H. Okuda, N. Takahashi, T. Miyata, "Starting current analysis of three-phase squirrel-cage induction motor by finite element method", Electrical Engineering in Japan, Vol. 99, pp. 36–42, 1979.

*[2] J. Buksnaitis,* "Analytical Determination of Mechanical Characteristics of Asynchronous Motors by Varying the Electric Current Frequency", Electronics and Electrical Engineering (Elektronika ir Elektrotechnika), Vol. 112, pp. 3-6, 2011.

[3] Z. Yongchang, Z. Jianguo, Z. Zhengming, Xu Wei, D.G. Dorrell, "An improved direct torque control for three-level inverter-fed induction motor sensorless drive", IEEE Transactions on Power Electronics, Vol. 27, pp. 1502 - 1513, Mar. 2012.

[4] R. Natarajan, V.K. Misra, M. Oommen, "Time domain analysis of induction motor starting transients", In Proc. 21st Annual North-American Power Symposium, Vol. 17, pp. 120-128, October 1989.

[5] S. Jangjit, P. Laohachai, "Parameter estimation of three-phase induction motor by using genetic algorithm", Journal of Electrical Engineering & Technology, Vol. 4, No. 3, pp. 360-364, 2009.

[6] S.R. Shaw, S.B. Leeb, "Identification of induction motor parameters from transient stator current measurements", IEEE Transactions on Industrial Electronics, Vol. 46, No. 1, pp. 139-149, Feb. 1999.

[7] Z. Nasiri-Gheidari, H. Lesani, "Using stator discharge current for the parameter estimation of a single-phase axial flux induction motor", Scientia Iranica, Vol. 19, No. 6, pp. 1794-1801, Dec. 2012.

[8] D. Lindenmeyer, H.W. Dommel, A. Moshref, P. Kundur, "An induction motor parameter estimation method", International Journal of Electrical Power & Energy Systems, Vol. 23, No. 4, pp. 251-262, May 2001.

[9] M. Stocks, A. Medvedev, "Estimation of induction machine parameters at start-up using current envelope", in Proc. IEEE 37th IAS Annual Meeting, Conference Record of the Industry Applications Conference, Vol. 2, pp. 1163-1170, Oct. 2002.
[10] S. Aksoy, A. Muhurcu, H. Kizmaz, "State and parameter estimation in induction motor using the Extended Kalman Filtering algorithm", In Proc. International Symposium on Modern Electric Power Systems (MEPS), pp. 1-5, Sep. 2010.
[11] J. Luszcz, "Motor cable effect on the converter-fed AC motor common mode current", PRZEGLA˛D ELEKTROTECHNICZNY (Electrical Review), Vol. 88, pp. 177-181, Jan. 2012.
[12] M.K. Kirar, G. Aginhotri, "Cable sizing and effects of cable length on dynamic performance of induction motor", IEEE Fifth Power India Conference, Murthal, India, Dec. 2012.
[13] A. Ketabi, I. Sadeghkhani, "Electric power systems simulation using MATLAB", 3rd Edition, Morsal Publications Allameh Feiz Kashani Institute of Higher Education Publications, Kashan, Iran, Feb. 2014. (in Persian)
[14] P.C. Krause, O. Wasynczuk, S.D. Sudhoff, S. Pekarek, "Analysis of electric machinery and drive systems", 3rd Edition, Wiley-IEEE Press, Jul. 2013.
**[15] I. Sadeghkhani**, A. Ketabi, R. Feuillet, "Investigation of transmission line models for switching overvoltages studies", Int. J. of Emerging Electric Power Systems, Vol. 14, pp. 231-238, July. 2013.
[16] L. Wang, C.N. M. Ho, F. Canales, J. Jatskevich, "High-frequency modeling of the long-cable-fed induction motor drive system using TLM approach for predicting overvoltage transients", IEEE Transactions on Power Electronics, Vol. 25, pp. 2653 – 2664, Oct. 2010.
[17] [Online]. Available: www.valiadis.gr/pool/ftp/drawings/KHV355-2_200KW_3300V_TEST_REPORT.pdf.
[18] P.C. Sen, "Principles of electric machines and power electronics", 2nd Edition, John Willey, Jan. 1997.
[19] C. Yildiz, S. Gultekin, K. Guney, S. Sagiroglu, "Neural models for the resonant frequency of electrically thin and thick circular microstrip antennas and the characteristic parameters of asymmetric coplanar waveguides backed with a conductor", AEU - International Journal of Electronics and Communications, Vol. 56, pp. 396–406, 2002.
[20] S. Haykin, "Neural network: A comprehensive foundation", 2nd ed., Prentice Hall, Upper Saddle River, NJ, USA, 1998.
[21] I. Sadeghkhani, A. Ketabi, "Switching overvoltages during restoration: Evaluation and control using ANN", Lambert Academic Publishing, Köln, Germany, Aug. 2012.
[22] R. Bayindir, S. Sagiroglu, I. Colak, "An intelligent power factor corrector for power system using artificial neural networks", Electric Power Systems Research, Vol. 79, pp. 152–160, 2009.
[23] S. Bunjongjit, A. Ngaopitakkul, "Selection of proper artificial neural networks for fault classification on single circuit transmission line", International Journal of Innovative Computing, Information and Control, Vol. 8, pp. 361-374, 2012.
[24] M.T. Hagan, M.B. Menhaj, "Training feedforward networks with the Marquardt algorithm", IEEE Trans. Neural Network, Vol. 5, pp. 989-993, Nov. 1994.